ISSN 2179-3956

FRICTION PROPERTIES OF NEW FLUORINATED CARBON PHASES[1]

PhilippeThomas[2]
Jean-LouisMansot[3]
O. Gros[4]
L. Legras[5]
Marc Dubois[6]
Katia Guérin[6]
André Hamwi[6]

Abstract
The present work is concerned with the understanding of the tribologic behaviour of various fluorocarbon phases (graphite fluorides, fluorinated carbon nanofibres and carbon nanodiscs/nanocones). The intrinsic tribologic properties of the studied compounds are correlated to their structure and chemical composition (F/C ratio, C-F bonding type) in order to deduce the parameters monitoring the friction behaviour. In all cases the friction properties of the fluorinated derivatives are better than those of the initial carbon compounds. In the case of fluorinated carbon nanofibres, the friction improvement is attributed to the interfibres interactions reduction resulting from surface free energy decrease induced by the fluorination of superficial graphene layers. For fluorinated carbon nanodiscs/nanocones bulk structural effects are predominent as far as the lowest friction coefficients are obtained for fluorinated derivatives of initial graphitized nanoparticles. This bulk effect is confirmed by the graphite fluorides tribologic behaviours. In these last cases a supplementary improvement is associated to the presence of intercalated mineral fluorides in the graphite van der Waals gaps.
Keywords : Solid lubricants; Fluorinated compounds ; Raman spectroscopy.

[1] *Technical contribution to the First International Brazilian Conference on Tribology – TriboBr-2010, November, 24th-26th, 2010, Rio de Janeiro, RJ, Brazil.*
[2] *Groupe de Technologie des Surfaces et Interfaces (GTSI), EA 2432, Faculté des Sciences Exactes et Naturelles, Université des Antilles et de la Guyane, 97159 Pointe à Pitre Cedex (France)*
[3] *Groupe de Technologie des Surfaces et Interfaces (GTSI), EA 2432, / Centre Commun de Caractérisation des Matériaux des Antilles et de la Guyane (C3MAG), Faculté des Sciences Exactes et Naturelles, Université des Antilles et de la Guyane, 97159 Pointe à Pitre Cedex (France)*
[4] *Centre Commun de Caractérisation des Matériaux des Antilles et de la Guyane (C3MAG) / Systématique-Adaptation-Evolution UMR 7138, Equipe « Biologie de la mangrove », Faculté des Sciences Exactes et Naturelles, Université des Antilles et de la Guyane, 97159 Pointe à Pitre Cedex (France)*
[5] *EDF - R&D, MAI, Avenue des Renardières, Les Renardières, 77818 Moret sur Loing Cedex*
[6] *Laboratoire des Matériaux Inorganiques, Université Blaise Pascal de Clermont-Ferrand, UMR CNRS-6002, 63177 Aubière (France)*

ISSN 2179-3956

1 INTRODUCTION

When two contacting solid bodies are moving one against the other, friction and wear processes occur leading to energy losses and mechanical failures.

In order to reduce these negative effects, in dynamic mechanical assemblies, lubricants (solids, gels or liquids) are introduced to avoid direct interaction between contacting surfaces.[1,2]

In the most severe lubrication regime, the boundary one, friction and wear reduction are associated to the action of friction reducers and antiwear additives introduced in the lubricating oils or greases.[3,4] The protective action of these additives results from the building, by chemical reaction between additives molecules and metallic substrates, of a tribofilm on the sliding surfaces.[3-10]

Such action mechanisms lead to a film formation time and a protective efficiency modulated by the reactivity of the additives with the sliding surfaces. In order to overcome these limitations, new strategies consisting in the introduction of nanoparticles of tribo-active phases (MoS_2, graphite, boron nitride,…) or tribo-active precursors (reverse micelles, carbon onions, inorganic fullerenes) are investigated.[11-20] In these cases, the nanoparticles are subjected to build immediately, in the sliding contact conditions, the protective tribofilm without any reaction with the substrates.

As fluorinated carbons and hydrocarbons are known as good friction and wear reducers,[21-24] this work is concerned with the study of the tribologic behaviour of new synthetized micro and nanoparticles of fluorinated carbon phases[25-29] subjected to be introduced as nano-additives in liquid or gel lubricants. Correlations between the structure, the chemical composition and the tribologic properties of fluorinated graphites, carbon nanodiscs and nanocones, carbon nanofibres are investigated in order to determine the structural and chemical parameters monitoring the friction properties of the various fluorinated carbon phases studied.

2 EXPERIMENTAL

2.1 Materials

Fluorinated graphites are prepared from Madagascar natural graphite powder at room temperature under F_2 atmosphere with a gaseous mixture of HF and a volatile fluoride to improve the reactivity of fluorine with graphite.[26] The volatile fluorides MF_n used are BF_3 and ClF_3 , leading to the fluorinated materials noted B and C respectively. The reaction time is 14h. The synthesis method is precisely described elsewhere.[26-29] The compounds are then treated under fluorine atmosphere at temperatures, noted T_{FPT}, ranging from 150 to 600°C leading to two series of compounds, named B(T_{FPT}) and C (T_{FPT}).

The second type of fluorinated compounds is obtained from high purity carbon nanofibres, noted CNFs, fluorinated at temperatures (T_F) ranging between 380°C and 472°C in F_2 atmosphere for a reaction time of 16h.[30] This allows to achieve fluorination contents, expressed as atomic F:C ratio, in the range 0.04-1.0.

The last type of materials consists of a mixture of nanodiscs (≈70% w/w), nanocones (≈20% w/w) and amorphous carbons (≈10% w/w). The initial mixture is called CNDs. Two series of fluorinated carbon nanodiscs/nanocones are prepared from as-product CNDs and CNDs heat-treated at 2700°C under argon in order to increase the mean range order (graphitization degree). The samples are then called

ISSN 2179-3956

CND2700s. The fluorination is performed in F_2 atmosphere for a reaction time of 3h at temperatures ranging from 280°C to 450°C for CNDs and from 450°C to 520°C for CND2700s.(31) The fluorination temperatures are selected to obtain similar fluorine contents for CNDs and CND2700s, allowing us to study the evolution of the tribologic properties as a function of F/C ratio. The F/C ratio is determined by two methods: ^{19}F NMR and measurement of the sample mass before and after fluorination (weight uptake method).

2.2 Tribological Tests

The tribologic properties of the compounds are evaluated using an alternative sphere-on-plane tribometer. The experimental conditions of the tribologic tests are summarized in Table 1.

The balls are used as delivered. The planes are polished to generate significant roughness needed to improve the adherence of the tested materials. The balls and the planes are cleaned in ultrasonic baths in acetone and ethanol in order to eliminate pollutants and remaining abrasive particles.

The surface roughnesses of balls and planes are measured using an optical Altisurf 500 profilometer (resolution 10 nm). The typical 2D (R_a) and 3D (S_a) roughness parameters are reported in Table 1.

The studied materials are deposited on the planes in the form of films by the burnishing method consisting in the crushing of few milligrams of powdery of fluorinated material between two planes leading to the formation of an adherent surface film of 1-2 μm thickness (measured using the optical Altisurf 500 profilometer) and 5 mm^2 area on each plane.

The intrinsic friction properties are investigated under air atmosphere (relative humidity: 50±5%) at 298 ±1K. The friction coefficient is determinated after three cycles which corresponds to the intrinsic tribologic properties of the deposited film, i.e. before structural transformations induced by the friction process.

Table 1: Experimental parameters of the tribologic tests

Steel ball	AISI 52100 stainless steel Hv = 850 Reduced Young modulus *E* = 210 GPa Diameter: 9.5 mm Roughness: R_a = 90 ± 10 nm ; S_a = 120 nm
Steel plane	AISI 52100 stainless steel, Hv= 850 Reduced Young modulus *E* = 210 GPa Diameter: 10 mm Roughness: R_a = 350 ± 10 nm ; S_a = 405 nm
Normal load	10 N
Contact diameter (Hertz's theory)	140 μm
Mean contact pressure	0.65 GPa
Sliding speed	6 $mm.s^{-1}$

2.3 Raman Investigations

Raman microspectrometry analyses of the initial compounds and of the tribofilms at the end of the friction tests are performed using a HR 800 Horiba multi channel spectrometer fitted with a Peltier cooled CCD detector for spectra recording. The exciting monochromatic light used is the 532 nm wavelength line delivered by a solid Nd YAG laser. The pre-monochromator is a notch filter and the monochromator

ISSN 2179-3956

a 300 lines/mm holographic grating. Our experimental conditions (objective lens x10, confocal hole 500µm, spectrometer entry aperture 500µm) lead to a probe diameter of 10 µm, a wavenumber resolution of 1.5 cm^{-1}. The laser power at the sample surface is 30 mW and the acquisition time is in the range of 10 to 60 seconds depending on the sample thickness. Special attention is paid to avoid sample irradiation damages during the analyses. In order to determine with a high precision Raman bandshifts resulting from structure evolutions, the samples are simultaneously illuminated with a vapour mercury lamp. Emission lines appearing at 1464 cm^{-1} and 1527 cm^{-1} are used as internal spectral references and allow to deduce the Raman band position with a precision of ± 1 cm^{-1}.

2.4 Transmission Electron Microscopy Investigations

The fluorinated nano fibers are first embedded in epon araldite. Thin slices (50-60 nm thick) are then obtained by means of ultramicrotomy (Ultracut E Leica microtome) using a diamond knife (Diatome AG) and deposited onto copper support grids.

Transmission electron microscopy investigations are carried out on a Tecnai F20 FEI electron transmission microscope fitted with an EDS link SiLi dectector for X rays analyses. The microscope is running at 200kV as acceleration voltage with a field emission extraction potential of 4500 V.

Transmission bright field and high resolution micrographs are recorded in TEM mode whereas the EDS profiles are collected in Scanning Transmission Electron Microscopy (STEM) mode using an electron probe of 2 nm diameter.

3 RESULTS

3.1 Graphite Fluorides

3.1.1 Chemical and structural investigations

The structural characterization shows that the room temperature fluorination of graphite leads to compounds in which all van der Waals gap are occupied by fluorine atoms and mineral fluorides catalysts (stage 1 GICs).[26,27] The thermal post-treatment under fluorine atmosphere induces structural evolutions of the compounds. The planar graphitic structure is maintained for T_{FPT}s < 350°C. The increase of T_{FPT} induces a progressive removal of intercalated catalysts, leading to the conversion of planar carbon cycles into armchair ones. This structural evolution is schematically presented in Figure 1.

Figure 1: Schematic representation of the structure evolution of the fluorinated compounds as a funtion of post treatment temperature: a) graphitic b) biphasic and c) armchair structures.

ISSN 2179-3956

The evolutions of the fluorine content and of the interlayer spacing are given in Table 2. For T_{FPT} < 450°C, the F/C ratio corresponds to fluorine semi-ionically and covalently bonded to carbon atoms but also to intercalated catalysts. The proportion of chemically bonded fluorine (semi-ionic, covalent) increases when the post-treatment temperature increases. Above 350°C the covalent C-F bonds fraction increases to the detriment of semi-ionic C-F bonds.

Raman spectroscopy analyses were performed on the materials before the friction tests. The spectra recorded on B(T_{FPT}) and C(T_{FPT}) compounds, in the wave number range 1000-1800 cm^{-1}, are presented in Figure 2. They exhibit mainly two Raman bands around 1350 cm^{-1}, associated to disorder, and 1600 cm^{-1} due to the overlap of characteristic G (graphite E_{2g} vibration mode at 1580 cm^{-1}) and disorder D' (1620 cm^{-1}) bands classically observed on the Raman spectra of carbonaceous materials presenting graphitic micro/nano domains.[32-34] The two previous Raman bands do not appear in the Raman spectra recorded on B(500) and B(550) fluorinated derivatives. It underlines the absence of aromatic groups and indicates that the structure is totally composed of puckered fluorocarbon layers (the carbon atoms only present sp^3 hybridization state).

Table 2: Evolution of the fluorine content (atomic F/C ratio determined from weight uptake) and interlayer spacing (deduced from XRD patterns) [26, 27] as a function of T_{FPT} for B (synthetized with HF-BF_3 catalysts) and C (synthetized with HF-ClF_x catalysts) series

Fluorination post-treatment temperature (T_{FPT})	B serie		C serie	
	F/C ratio	d_{001} (nm)	F/C ratio	d_{001} (nm)
Room temperature	0.47	0.629	0.42	0.626
150°C	0.39	0.617	-	-
250°C	0.40	0.620	0.41	0.623
300°C	0.41	0.621	0.43	0.630
350°C	0.63	0.621	0.45	0.632
400°C	0.85	0.655	0.51	0.643
450°C	0.93	0.701	0.80	0.693
500°C	0.99	0.734	0.93	0.718
550°C	1.01	0.702	0.94	0.720

The structural influence of fluorination is characterized on the spectra by an increase of the relative intensities of D and D' modes and a downshift of the D band as T_{FPT} (and consequently the chemically bonded fluorine fraction) increases. This evolution has already been observed for other fluorinated compounds and attributed to both the size reduction of graphitic domains and the yield increase of C-F covalent bonds.[26,33-34]

ISSN 2179-3956

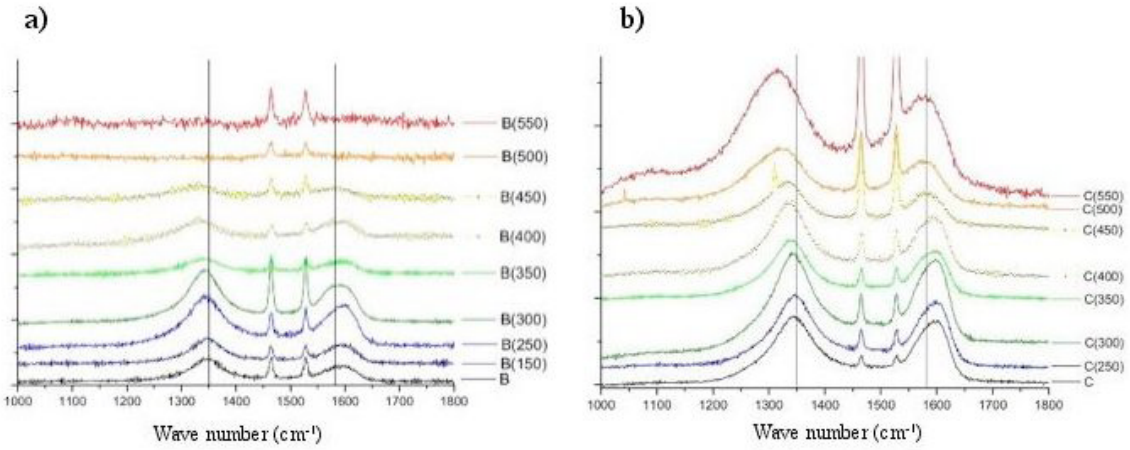

Figure 2: Raman spectra recorded on a) B(T_{FPT}) and b) C(T_{FPT}) compounds. The two thin bands at 1464 cm^{-1} and 1527 cm^{-1} are the emission lines of a vapour mercury lamp used as internal standard for accurate determination of the Raman bandshifts.

According to Knight and White relation,[34] $L_a = 44\frac{I_G}{I_D}$, the graphitic nano domains spatial extension L_a (parallel to graphene layers) can be deduced from the relative intensities of D and G bands. The evolutions of L_a as a function of T_{FPT} are given in Figure 3. The size of the graphitic domains does not evolve as far as catalysts species are still intercalated in the structure. The removal of catalysts (T_{FPT}s > 350°C) leads to a drastic decrease of L_a due to the increase of the covalent C-F bonds content associated to the desappearance of planar carbon cycles.

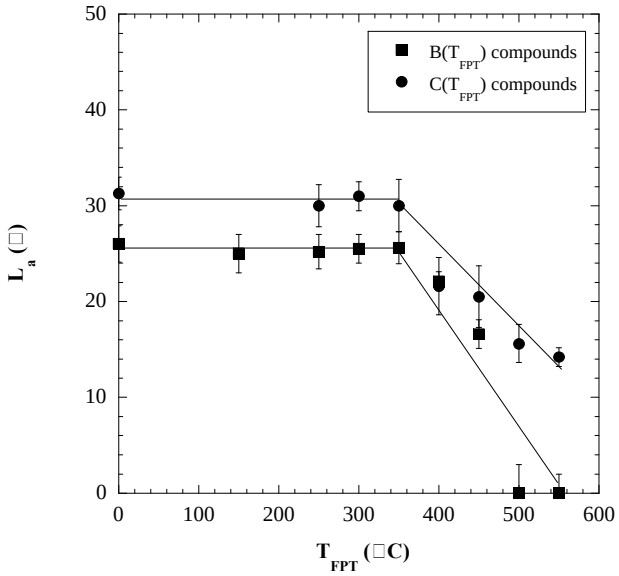

Figure 3: Evolution of L_a coherence length (size of the graphitic domains) as a function of post-treatment temperature.

3.2 Friction Properties

The friction coefficients obtained for the various fluorinated materials at the beginning of the tribological test (3 cycles) are presented in figure 4 as a function of fluorination post-treatment temperature. The compounds all present good intrinsic friction properties, better than pristine graphite. The lowest friction coefficients are

ISSN 2179-3956

obtained for low and intermediate fluorination temperatures as μ remains stable (μ = 0.055 and μ = 0.06 for B and C series respectively) for the room temperature synthesized compounds and the post-treated ones at T_{FPT}s < 450°C. An increase of μ is observed for T_{FPT}s > 500°C up to 0.08 and 0.1 for B and C materials respectively.

The correlation of the friction results and structural characterizations of the fluorinated compounds shows that high friction coefficients are obtained for perfluorinated derivatives which structure is characterized by puckered fluorocarbon layers (armchair conformation of carbon cycles corresponding to covalent C-F bonds).[36,37] The best tribological results are observed for compounds presenting graphitic or biphasic structures, i.e. if the graphitic structure is partially maintained. The Figure 5 clearly emphasizes a relationship between the friction properties of graphite fluorides and the size of the remaining graphitic domains.

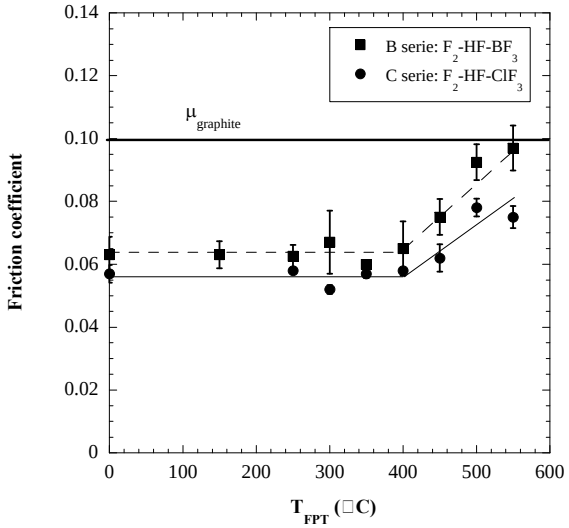

Figure 4: Evolution of friction coefficient (recorded after three cycles) as a function of fluorination post-treatment temperature for B(T_{FPT}) and C(T_{FPT}) materials.

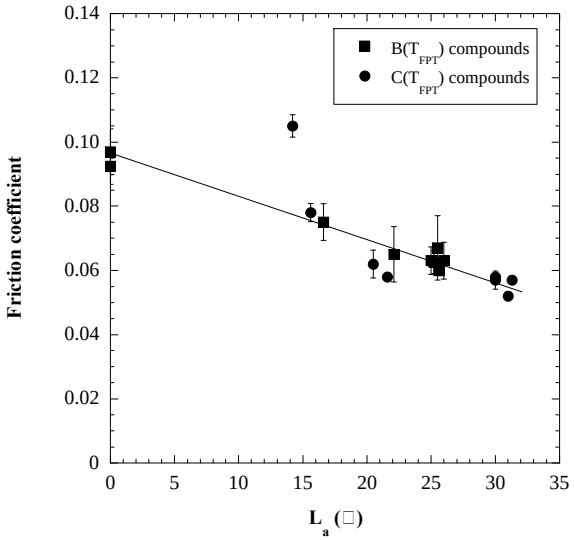

Figure 5: Evolution of friction coefficient (recorded after three cycles) as a function of L_a coherence length (size of the graphitic domains).

ISSN 2179-3956

3.3 Carbon Nanofibres

3.3.1 Structure of fluorinated CNFs

The direct fluorination of CNFs at temperature ranging between 420°C and 480°C leads to fluorinated carbon nanofibres with fluorine contents in the range 0.04 < F/C < 1.0 measured by ^{19}F NMR.[30] The increase of the fluorination temperature T_F leads to a progressive fluorination which processes from the outer part of the carbon nanofibre towards its core as emphasized by the transmission electron micrographs presented in Figure 6.

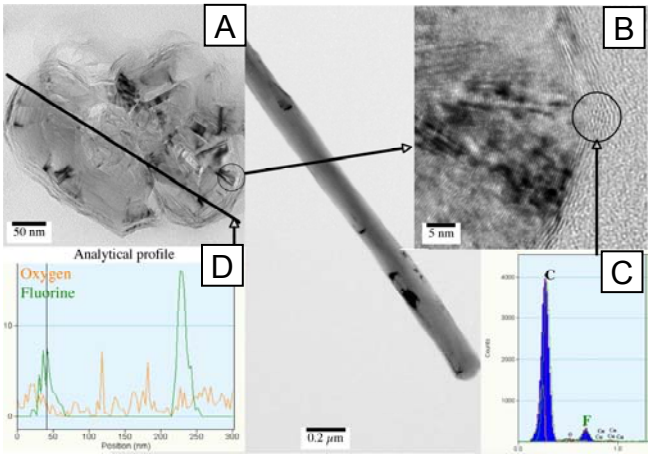

Figure 6: Analytical Transmission Electron Microscopy study of the cross section (A) of fluorinated carbon nanofibres with F/C= 0.2. Lattice fringes corresponding to graphitic structure are visible in the internal part of the fibre (B). The presence of fluorine at the periphery of the fiber is clearly pointed out either by the X-rays analysis profile (C) (D) or enhanced lattice fringes feature (B).

3.3.2 Friction properties

The tribologic properties of fluorinated CNFs are presented in Figure 7. The fluorination process strongly improves the friction properties as μ decreases from 0.13 for pristine CNFs down to 0.08 for F/C = 0.15 and does not evolve any more when increasing the fluorination rate (0.2-0.8 F/C range).

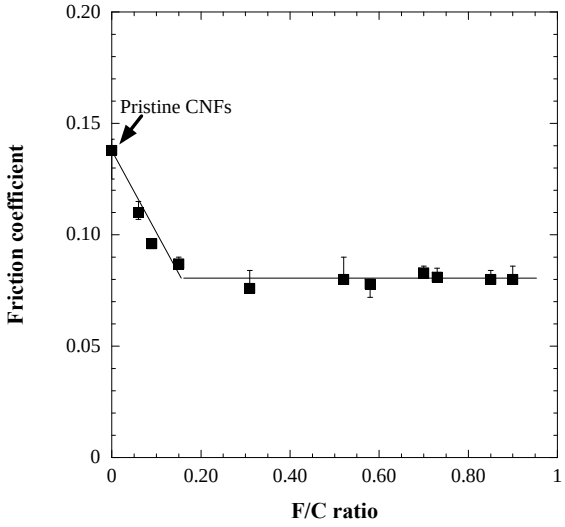

Figure 7: Evolution of friction coefficient of fluorinated carbon nanofibres as a function of the F/C ratio (determined by ^{19}F NMR[35]).

ISSN 2179-3956

In order to investigate the influence of the friction process on the structure of the materials, the tribofilms were studied by means of SEM and Raman spectroscopy experiments. The SEM micrographs collected on initial CNFs, on the tribofilm and on a particle of tribofilm extracted from the wear scar are shown in Figure 8 in the case of pristine nanofibres.

Figure 8b) clearly shows an orientation of the fibres along the sliding direction in the low contact pressure zone. The tribofilms of 1 μm thickness present a continuous surface which exhibits ondulations parallel to the sliding direction with sizes of the same order than CNFs diameters. The micrographs collected on a tribofilm particle (Figures 8c and 8d)) clearly show the fibrous nature of the film.

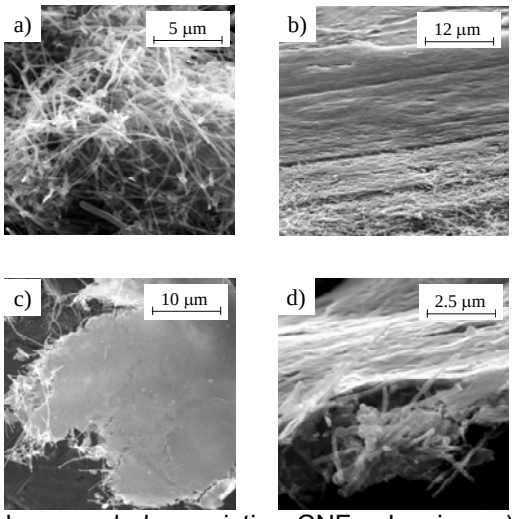

Figure 8: SEM micrographs recorded on pristine CNFs showing: a) tangled CNFs deposited on the plane out of the contact zone ; b) aspect of the tribofilm ; c) and d) particle of the tribofilm extracted from the wear scar.

3.4 Carbon Nanodiscs/Nanocones

3.4.1. Structure of the compounds

AFM and SEM investigations, performed on pristine and fluorinated CNDs and CND2700s,[31] are presented in Figure 9. The AFM and SEM pictures corresponding to pristine CNDs (Figures 9a, 9b and 9c) and CND2700s (Figures 9g, 9h and 9i) show that the main difference is related to the roughness of the nanodiscs/nanocones surfaces. In the case of CNDs, the surface roughness reveals a granular structure with grains of 30 nm of average spatial extension. In the case of CND2700s, the surface appears extremely smooth.[31] This can be attributed to the graphitization process leading to long range graphitic domains with basal graphene layers parallel to the nanodiscs surfaces. The AFM image reveals the presence of steps (underlined by arrows in the Figure 9h) probably corresponding to the boundaries of large graphitized domains. X-rays diffraction investigations carried out on initial CNDS and CND2700s reveal graphitic domains with spatial 2nm along C axis and 10 nm along graphene plane for CNDS and 40nm along C axis and 35 nm along graphene plane for graphitized CND2700s. These structure differences observed between the CNDs (granular structure with nanodomains) and graphitized CND2700s (large graphitic domains) is responsible of the higher reactivity of CNDs with fluorine (lower reaction temperature) than CND2700s.

ISSN 2179-3956

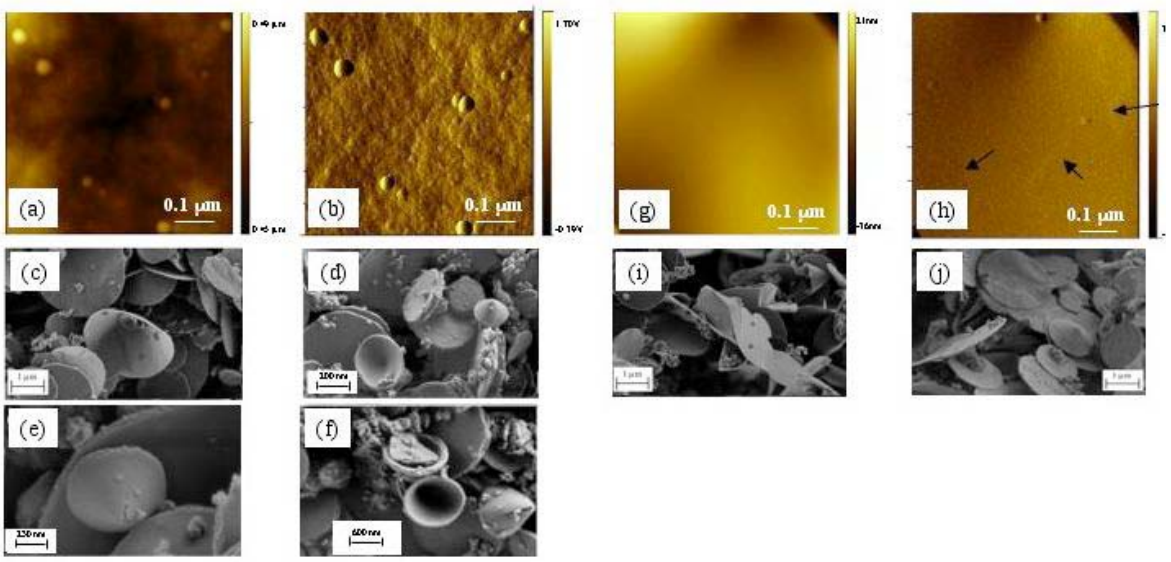

Figure 9: a), b) AFM micrographs recorded on initial CNDs and c) corresponding SEM micrograph ; d), e) SEM micrographs recorded on CND-340 , f) SEM micrographs recorded on CND-450 ; g), h), AFM images recorded on initial graphitized CND2700s and i) corresponding SEM micrograph ; j) SEM micrographs recorded on CND2700-500.[31]

3.4.2 Friction Properties

The intrinsic tribologic properties of fluorinated CNDs and CND2700s as a function of the fluorine content are presented in Figure 10. Initial non-fluorinated CNDs and CND2700s compounds present readily different behaviours. The friction coefficient of CNDs is more than two times larger than the CND2700s one. This can be attributed to the highly organized structure of CND2700 sample (large graphitic domains), compared to CNDs one which is constituted of tiny graphitic domains surrounded by amorphous zones.

The influence of fluorination is important for the CNDs as far as the friction coefficient decreases from 0.21 for initial CNDs down to 0.10 for high fluorine contents (F/C = 0.90). In the case of CND2700s, the influence of the fluorine content is weaker. As for graphite fluorides[38,39] the best tribologic performances ($\mu < 0.08$) are obtained for F/C ratios in the range 0.1-0.7, the friction coefficients for F/C > 0.7 being larger than the initial compound one.

ISSN 2179-3956

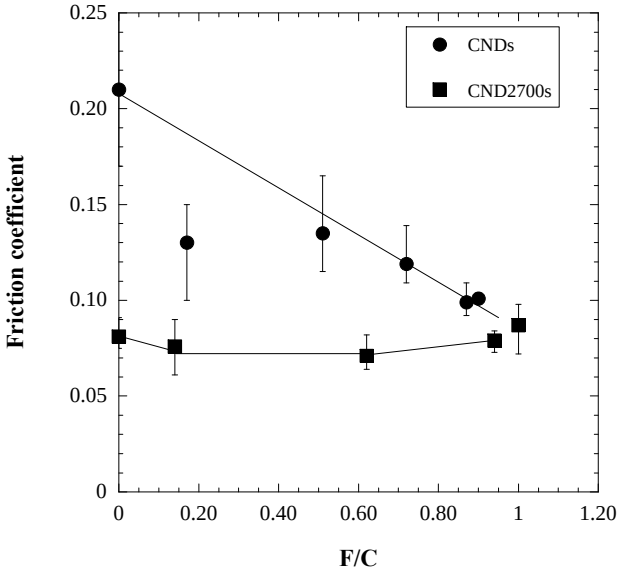

Figure 10: Evolution of intrinsic friction coefficient of fluorinated CNDs and CND2700s as a function of F/C ratio (determined from weight uptake and ^{19}F NMR).

4 DISCUSSION

The correlation between friction properties and structure evolutions of the fluorinated compounds points out different friction mechanisms.

In the case of fluorinated carbon nanofibres, the fibrous nature of the tribofilms observed suggests that individual nanofibres interactions are involved in the friction process. The progressive friction reduction for 0 < F/C < 0.15 proceeds via the lowering of the fibers surface free energy resulting from the fluorination of the external graphene layers as clearly shown by tranmission electron microcopy. The stabilization of the friction coefficient at 0.08 for F/C > 0.15 is attributed to the fact that the fluorination of the inner layers does not affect any more the surface free energy.

In the case of carbon nanodiscs/nanocones, drastic differences of tribologic behaviours between fluorinated derivatives obtained from ill organized nanoparticles and graphitized ones points out that for these particles the initial long range order (graphitic structure) is a parameter of first order in the friction reduction process. Pristine and fluorinated graphitized CND2700s present large graphitic domains (30 – 40 nm characteristic dimensions) with graphene layers parallel to the surfaces of the nanodiscs/nanocones. The preferential orientation of the nanoparticles in the sliding contact with their surfaces parallel to the friction surfaces leads to a preferential orientation of the graphitic domains with their graphene layers parallel to the sliding plane resulting in a low friction coefficient value (μ = 0.08). Indeed, the fluorination process modifies the corrugation of the carbon layers by fluorine atoms incorporation and carbon cycles conformation changes (planar to armchair conformation) but does not induce any crystallites orientation changes. In the case of CNDs, the higher friction coefficient (μ = 0.21) can be attributed to their ill organized structure. As revealed by morphologic and structural analyses, CNDs present two levels of organization. They are constituted of agglomerated nanograins (typical size 30 nm), each nanograin being composed of randomly oriented graphitic nanodomains (typical size 10x2 nm). The graphitic nanodomains do not present any preferential orientation relative to the surfaces of the nanodiscs/nanocones resulting in poor friction reduction properties. As previously mentionned, the fluorination process will not

ISSN 2179-3956

induce any orientation changes of the nanodomains. The improvement of friction properties can be mainly attributed to the reduction of nanograins interactions resulting from fluorination. As a consequence, contrarily to CNFs, the improvement of friction properties seems to result from bulk effects and are obtained for low fluorine contents.

This bulk effect is also at the origin of the friction mechanisms observed in the case of graphite fluorides. The correlation of the tribologic data to the Raman analyses carried out on the initial compounds points out that low friction coefficients are obtained when a lot of graphene planes are maintained. This corresponds to partially fluorinated compounds (Room Temperature < T_{FPT} < 450°C) where graphitic domains (fluorine atoms are semi-ionically bonded to aromatic rings) can coexist with perfluorinated ones (fluorine atoms covalently bonded to Csp^3 atoms). The change in the nature of the fluorine-carbon bonding from semi-ionic (planar aromatic graphene layers) to covalent (armchair conformation of non-aromatic carbon rings leading to puckered fluorocarbon layers) leads to a severe evolution of the friction properties. A rapid increase of the friction coefficient is correlated to the increase of C-F covalent bond concentration. This induces a decrease of the graphitic domains extension.

5 CONCLUSION

The investigations of the friction properties of pristine and fluorinated carbon phases shows a beneficial role of fluorination on the lubricating performances of the compounds. The obtained friction coefficients are as low as those of conventional fluorocarbon lubricants.

In the case of graphite fluorides, the bi-fluorination process (room temperature synthesis and post-treatment under fluorine atmosphere) allows to control the nature of the C-F bonding and as a consequence the friction properties.

The tested carbon nanostructures appear as promising new nano-additives. Here again, the control of the fluorination conditions allows to achieve the optimized friction properties. The advantages of the tested fluorinated nanocarbons are their sizes and geometries, well adapted for a good feeding of the sliding interface, their high chemical and temperature stability and the possibility to obtain stable dispersions in liquid or gel lubricants.

REFERENCES

1 Booser, E.R.: Tribology data handbook, CRC Press, New York (1997)
2 Georges, J.M.: Frottement, usure et lubrification: la tribologie ou science des surfaces, CNRS editions, Eyrolles (2000)
3 Martin, J.M.: Contribution à la tribologie: Etude du mécanisme d'action d'un additif anti-usure en régime de lubrification limite. Aspects chimiques dans le cas des organodithiophosphates métalliques, Thèse d'état n° 7827, Université Claude Bernard, Lyon (1978)
4 Mansot, J.L. , Terech, P., and Martin, J.M., "Structural investigation of lubricating greases" Colloids and Surfaces **39**, 321 (1989)
5 Martin, J.M., Mansot, J.L., Berbezier, I., Dexpert, H.: The nature and origin of wear particle from boundary lubrication with ZDDP. Wear **93**, 117-126 (1984)
6 Martin, J.M., Mansot, J.L., Berbezier, I., Belin, M.: Microstructural aspects of lubricated mild wear with zinc dithiophosphate. Wear **107**, 355-366 (1986)
7 Martin, J.M., Belin, M., Mansot, J.L.: Friction induced amorphization with ZDDP. An EXAFS study. ASLE Transactions **49**, 523-531 (1986)

ISSN 2179-3956

8 Bell, J.C., Delargy, K.M., Seeney, A.M.: The removal of substrate material through thick zinc dithiophosphate antiwear films. In Dowson, D. (ed.), Tribology series, 21, wear particles: from the cradle to the grave, Elsevier, Amsterdam, pp. 387-396 (1992)
9 Martin, J.M., Grossiord, C., Lemogne, T., Bec, S., Tonck, A.: The two layers structure of Zndtp tribofilm part 1: AES, XPS and XANES analyses. Tribol. Int. **31**, 627-644 (2001)
10 Martin, J.M.: Lubricant additives and the chemistry of rubbing surfaces: metal dithiophosphates triboreaction films revisited. Jpn. J. Tribol. **42**, 724-729 (1997)
11 Fleishauer, P.D., Lince, J.R., Bertrand, P.A., Bauer, R.: Electronic structure and lubrication properties of MoS_2: a quantitative molecular approach. Langmuir **5**, 1009 (1989)
12 Zaidi, H., Robert, F., Paulmier, D.: Influence of adsorbed gases on the surface energy of graphite: consequences on the friction behaviour. Thin solid films **264**, 46-51 (1995)
13 Mansot, J.L., Hallouis, M., Martin, J.M.: Colloidal antiwear additives. Part one: Structural study of overbased calcium alkylbenzene sulfonate micelles. Colloids and Surfaces **A 71**, 123-134 (1993)
14 Mansot, J.L., Hallouis, M., Martin, J.M.: Colloidal antiwear additives. Part two: Tribological behaviour of colloidal additives in mild wear regime. Colloids and Surfaces **A 75**, 25-31 (1993)
15 Joly-Pottuz, L., Dassenoy, F., Martin, J.M., Vrbanic, D., Mrzel, A., Mihailovic, D., Vogel, W., Montagnac, M.: Tribological properties of Mo-S-I nanowires as additive in oil. Tribol. Lett. **18**, 385-393 (2005)
16 Joly-Pottuz, L., Dassenoy, F., Belin, M., Vacher, B., Martin, J.M., Fleischer, N.: Ultralow friction and wear properties of IF-WS2 under boundary lubrication. Tribol. Lett. **18**, 477-485 (2005)
17 Mansot, J.L., Golabkan, V., Romana, L., Césaire, T. : Chemical and physical characterization by EELS of strontium hexanoate reverse micelles and strontium carbonate nanophase produced during tribological experiments. J. of Micr. **210**, 110 (2003)
18 Mansot, J.L., Golabkan, V., Romana, L., Bilas, P., Alleman, E., Bercion, Y.: Tribological and physicochemical characterization of strontium colloidal additives in mild wear regime. Colloids and Surfaces **A 243**, 67-77 (2004)
19 Nanolubricants, Tribology Series, Martin, J.M., Ohmae O. ed., Wiley, New York (2008**)**
20 Mansot, J.L., Martin, J.M., Bercion, Y., Romana, L.: Nanolubrication, Brazilian J. of Physics. **39**, 186-197 (2009)
21 Hirata, A., Igarashi, M., Kaito, T.: Study of solid lubricant properties of carbon onions produced by heat treatment of diamond clusters or particles. Tribol. Int. **37**, 899-905 (2004)
22 Fusaro, R.L., Sliney, H.E.: Graphite fluoride $(CF_x)_n$. A new solid lubricant. ASLE Trans. **1**, 56-75 (1970)
23 Fusaro, R.L.: Mechanisms of graphite fluoride $(CF_x)_n$ lubrication. Wear **53**, 303-323 (1979)
24 Tsuya, Y.: Tribology of graphite fluorides. in T. Nakajima (Ed), Fluorine-carbon and fluoride-carbon materials, Marcel Dekker, New York, pp. 355-380 (1995**)**
25 Kita, Y., Watanabe, N., Fuji, Y.: Chemical composition and crystal structure of graphite fluoride. J. of American Chemical Society **101**, 3832-3841 (1979)
26 Hamwi, A., Daoud, M., Cousseins, J.C.: Graphite fluorides prepared at room temperature. 1. Synthesis and characterization. Synthetic Metals **26**, 89-98 (1988)
27 Hamwi, A.: Fluorine reactivity with graphite and fullerenes. Fluoride derivatives and some practical electrochemical applications. J. of Physics and Chemistry of Solids **57**, 677-688 (1996)
28 Delabarre, C., Guérin, K., Dubois, M., Giraudet, J., Fawal, Z., Hamwi, A.: Highly fluorinated graphite prepared from graphite fluoride formed using BF_3 catalyst. J. Fluorine Chemistry, **126**, 1078 (2005)

ISSN 2179-3956

29 Delabarre, C., Dubois, M., Guérin, K., Fawal, Z., Hamwi, A.: Room temperature graphite fluorination process using chlorine as catalyst. J. Physics and Chemistry of Solids, **67**, 1157 (2006)
30 Chamssedine, F., Dubois, M., Guérin, K., Giraudet, J., Masin, F., Ivanov, D.A., Vidal, L., Yazami, R., Hamwi, A.: Reactivity of carbon nanofibers with fluorine gas. Chem. Mater **19**, 161-172 (2007)
31 Zhang, W., Moch, L., Dubois, M., Guérin, K., Giraudet, J., Masin, F., Hamwi, A.: Direct fluorination of carbon nanocones and nanodiscs. J. Nanosc. Nanotech. **8**, 1-6 (2008)
32 Dresselhaus, M.S., Dresselhaus, G., Advances in Physics, **51**, 1 (2002)
33 Dresselhaus, M.S., Pimenta, M.A., Ecklund, P.C., Dresselhaus, G., Raman scattering in material science, W.H. Weber and R. Merlin (eds), Springer, New York, 315 (2000)
34 Merlin, R., Pinczuk, A., Weber, W.H., Raman scattering in material science, W.H. Weber and R. Merlin (eds), Springer, New York, 1 (2000)
35 Knight, D.S., White, W.B.: Characterization of diamond films by Raman spectroscopy. J. Mater. Res. **4**, 385-393 (1989)
36 Rao, A.M., Fung, A.W.P., di Vittorio, S.L., Dresselhaus, M.S., Dresselhaus, G., Endo, M., Oshida, K., Nakajima, T.: Raman scattering and transmission-electron-microscopy studies of fluorine-intercalated graphite fibers C_xF ($7.8 \geq x \geq 2.9$). Phys. Rev. B **45**, 6883-6892 (1992)
37 Gupta, V., Nakajima, T., Ohzawa, Y., Zemva, B.: A study on the formation of graphite fluorides by Raman spectroscopy. J. Fluor. Chem. **120**, 143-150 (2003)
38 Thomas, P., Delbé, K., Himmel, D., Mansot, J.L., Cadoré, F., Guérin, K., Dubois, M., Delabarre, C., Hamwi, A.: Tribological properties of low-temperature graphite fluorides. Influence of the structure on the lubricating performances. J. Phys. Chem. Solids **67**, 1095-1099 (2006)
39 Delbé, K., Thomas, P., Himmel, D., Mansot, J.L., Dubois, M., Guérin, K., Delabarre, C., Hamwi, A. : Tribological properties of room temperature fluorinated graphite heat-treated under fluorine atmosphere, Tribol. Lett., **37**(1), 31-41 (2010)
40 Thomas, P., Himmel, D., Mansot, J.L., Dubois, M., Guérin, K., Zhang, W., Hamwi, A.:Tribological properties of fluorinated carbon nanofibres. Tribol. Lett., **34**, 49-59 (2009)